Project Portfolio

Investigation of Robust Controller Design in Microgrid for Effective Power Transfer

July 2025

Dhikshanya S
Electrical and Electronics Engineering Graduate
SRM Institute of Science and Technology

Key Areas:

Power Electronics | Embedded Systems | FPGA | Microgrid Control | Renewable Energy

Contact: www.linkedin.com/in/dhikshanya20,s.dhikshanya432@gmail.com

1. Project Overview

This project focuses on advanced control strategy for a grid-forming inverter in a grid-connected microgrid system with renewable energy sources. The system under study includes a solar photovoltaic (PV) system combined with a Battery Energy Storage System (BESS), interfaced through a bidirectional DC-DC converter. The various inverter control topologies are explored, focusing particularly on droop and the Virtual Synchronous Machine (VSM) control approach to ensure grid stability and effective synchronization. The microgrid network, experiences switching transients during disturbances such as sudden load variations or fault conditions. These transients can degrade performance and affect overall system reliability. To address this, this project introduces a robust Sliding Mode Controller (SMC) aimed at minimizing switching transients under different operating scenarios. The SMC enhances dynamic response and ensures faster system stabilization. Different case studies are conducted to evaluate the performance of the proposed method under different fault and load conditions in a simulation environment Furthermore, the control strategies are validated through hardware implementation in a 1 kW microgrid setup. The experimental results confirm the effectiveness of the proposed sliding mode control in grid forming inverter in reducing transient and improving the operational reliability of grid-forming inverters in renewable-integrated microgrids.

2. Tools & Technologies

- MATLAB / Simulink
- VHDL
- Xilinx FPGA
- Embedded Systems
- Power Electronics Hardware

3. System Design

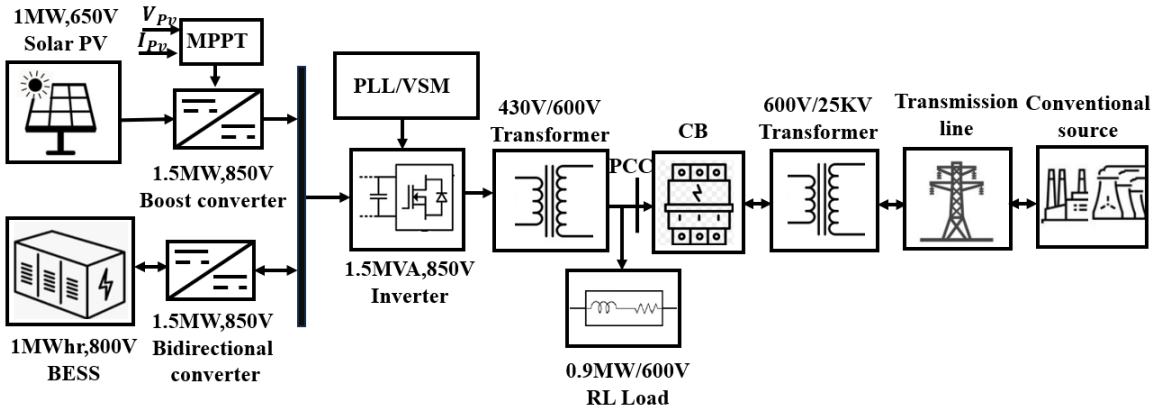

Fig .1.Block diagram of hybrid microgrid system

A simplified model of a microgrid-connected system is shown in Fig. 1. In this system, a photovoltaic (PV) system is integrated with the grid, and a battery energy storage system (BESS) is implemented through a bidirectional converter. A PI based voltage controller, regulates the battery's charging and discharging process. The battery stores energy from both the solar PV system and the grid, ensuring availability during periods of low solar irradiation or high energy demand. To increase the PV system's voltage, a boost converter is employed, along with a Maximum Power Point Tracking algorithm to optimize power extraction under varying weather conditions while maintaining a stable DC bus voltage. The MPPT uses the Perturb and Observe (P&O) algorithm to continuously track the PV panel's output voltage and current, ensuring maximum power generation. The system exhibits dynamic load characteristics, in grid-connected mode, the PV system generates maximum power, whereas, in islanded mode, it only produces enough power to meet the demand. A three-phase transformer facilitates step-up and step-down voltage conversion, while an AC load is connected at the Point of Common Coupling (PCC). A three-phase circuit breaker is used to transition between different operational modes.

4. Controller Strategy

4.1: Structure of grid following inverter controller

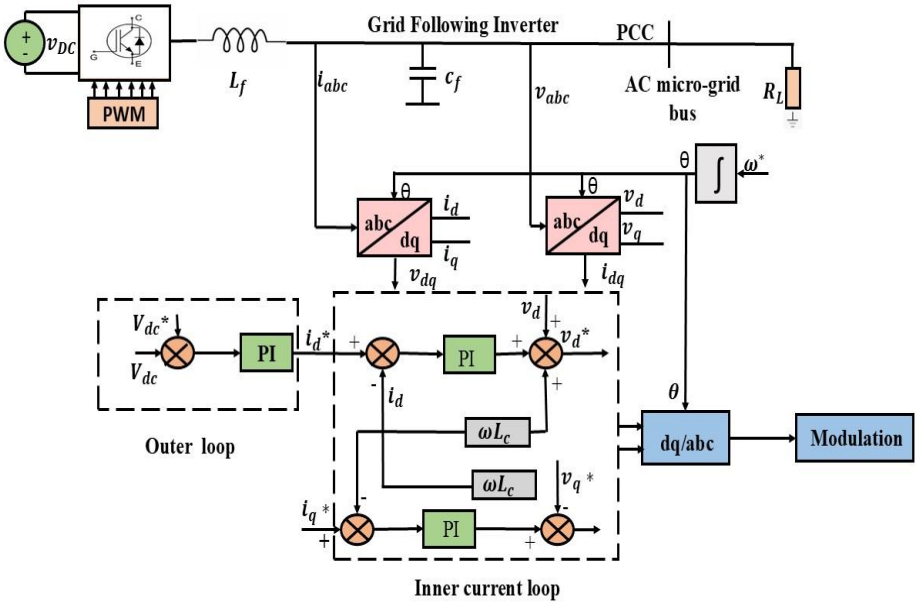

Fig .2. Block diagram of GFL controller

A grid-following (GFL) inverter operates as a voltage source, providing an output voltage reference. Which is shown in Fig. 2 The Phase-Locked Loop (PLL) continuously tracks the grid voltage phase angle, compares it with the generated signal, and produces an error signal proportional to the phase difference. The system then adjusts the frequency to minimize phase error and maintain grid synchronization. GFL inverters rely entirely on the grid for synchronization, making them incapable of independent operation when the grid is unavailable. The voltage control loop regulates the inverter voltage, using a Park transformation to convert the three-phase (abc) voltages into direct-quadrature (dq) components. The reference voltage (V^*)is converted into V_d* and V_q* and these values are compared with the actual voltages. The PI controller processes the error signal to regulate the output. Similarly, the current components (I_{abc}) are transformed into i_d and i_q, compared with their respective reference values (i_d*and i_q*), and processed by the PI controller. Using a Clarke transformation, the control signals (U_{abc}) are generated and converted into switching pulses for the inverter. While GFL inverters can operate in both grid-connected and islanded modes, they lack the capability to function independently when the grid is down. Their response time is relatively slow, and they have limited communication capabilities.

4.2: structure of grid forming inverter controller

The grid-forming Virtual Synchronous Machine (VSM) controller is used to manage voltage and frequency, emulating the behaviour of a synchronous generator. The VSM has the properties and dynamics of a typical synchronous generator, including virtual inertia that improves system stability. When there is a power imbalance, the VSM helps keep the system frequency within an acceptable range.

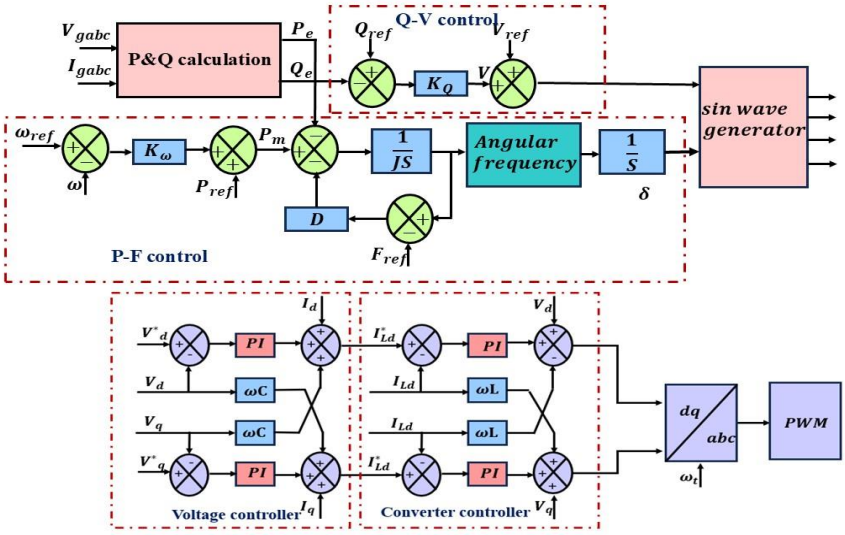

Fig. 3 Block diagram of Virtual synchronous machine inverter controller for microgrid

If power demand increases, the VSM injects inertia into the system, preventing the frequency from dropping below the threshold. Conversely, if demand decreases, the VSM absorbs inertia, preventing the frequency from exceeding the upper limit. This stored inertia acts as energy, playing a crucial role in reducing the Rate of Change of Frequency (RoCoF). The control of power and frequency is achieved using a power-frequency (P-F) control mechanism, as shown in Fig. 3. During islanded mode, the VSM injects reactive power into the system to regulate voltage at the Point of Common Coupling (PCC). A voltage and current controller is implemented to regulate system parameters and generate PWM signals for the inverter. By emulating the electromechanical characteristics of a synchronous generator, the VSM improves system stability, enhances transient response, and ensures smooth operation during grid disturbances.

4.3: Structure of sliding mode controller

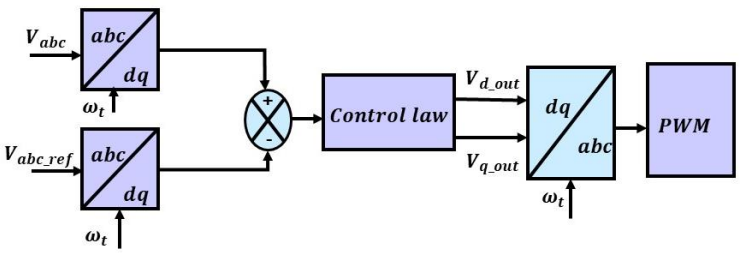

Fig.4 Sliding mode controller

Sliding Mode Control (SMC) Fig. 4 is a robust nonlinear control technique designed to ensure system stability and performance in the presence of uncertainties, disturbances, and nonlinearities. It operates by defining a sliding surface in the system‘s state space, where the desired dynamics are achieved. The control law in SMC typically consists of an equivalent control term to maintain the system on the sliding surface and a switching term to counteract disturbances and uncertainties. However, the discontinuous nature of the switching term often leads to chattering, which is mitigated using smoothing techniques like boundary-layer approximations. SMC is widely used in applications requiring high reliability in power systems, due to its ability to handle uncertainties and external disturbances effectively.

SMC control law as follow:

$$V_{d\_Out} = V_d^* - K * sat(S_d, \emptyset)$$

$$V_{q\_Out} = V_q^* - K * sat(S_q, \emptyset)$$

Where 'u' is the controller output, is reference output voltages of inverter controller, is sliding surface, is a sliding mode gain, and is saturation functions. The saturation ensures that the control signal stays within a desired boundary layers thickness. The role of SMC is to ensure robust and fast convergence of the system states to their desired values, even in the presence of uncertainties or disturbance.

5. Simulation Results

Case1: Grid to Islanded mode :

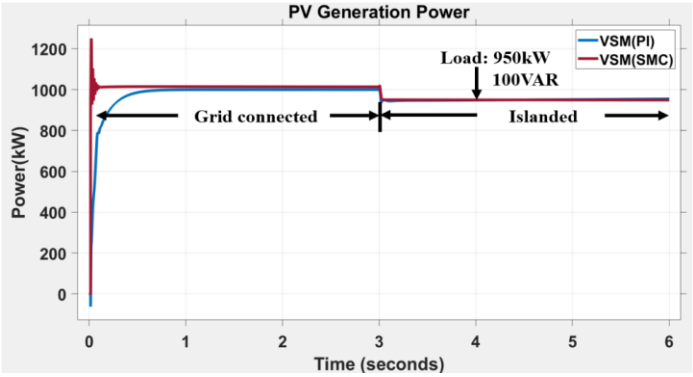

Fig.5 PV generation power

During the grid-connected mode with maximum irradiation and temperature, the PV generated a maximum power of 1 MW. From 0s to 3s, the PV was connected to the grid. As shown in Figure (5), the VSM with SMC settled at 0.1ms, whereas the VSM without SMC settled at 0.6ms. The SMC reduced the settling time by 0.5 times compared to the system without SMC. From 3s to 6s, the system operated in islanded mode. During this period, the generated power met the required load demand. The load demand was 950 kW, and according to the load characteristics, the PV generated the exact amount of power needed**.**

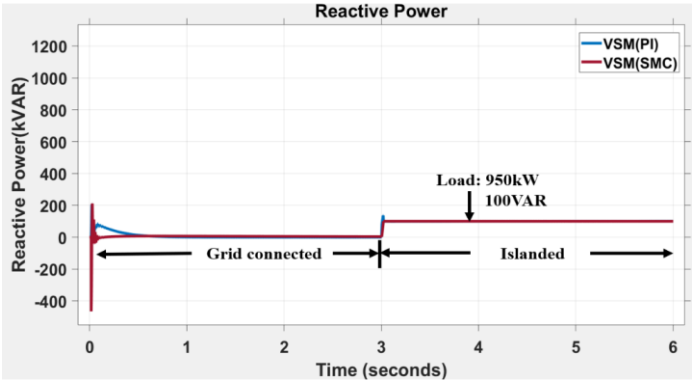

Fig.6 System reactive power

During the grid-connected mode with constant maximum irradiation and temperature, the PV generates maximum power. From 3s to 6s, the system operates in islanded mode. During this period, the VSM controller injects reactive power to maintain the system's voltage magnitude and ensure system stability. VSM with SMC the reactive power settled at 0.1ms whereas the VSM

without SMC settled 0.4ms as shown in Figure (6). The VSM adjusts the reactive power injection based on system conditions, helping to regulate voltage fluctuations and enhance stability. This capability is particularly essential in islanded mode, where the system lacks support from the main grid, making reactive power management vital for maintaining proper voltage profiles and overall system performance.

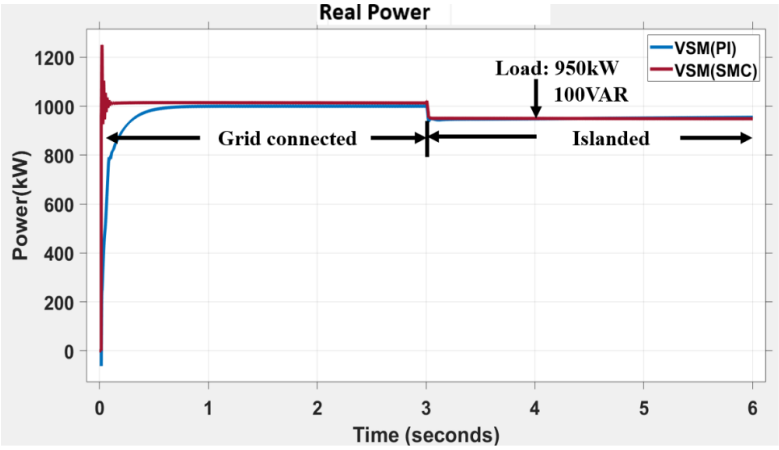

Fig.7 System Real power

During maximum irradiation and temperature, the transition from grid-connected mode to islanded mode is shown in Figure 7. The real power of the VSM without SMC initially experiences a switching transient of 1990 kW at 0.1ms and settles at 0.6ms. In contrast, the VSM with SMC experiences a switching transient of 1089 kW at 0.1ms from its operating power of 900 kW and settles at 0.1ms.From 0s to 3s, the system operates in grid-connected mode, and from 3s to 6s, it transitions to islanded mode.

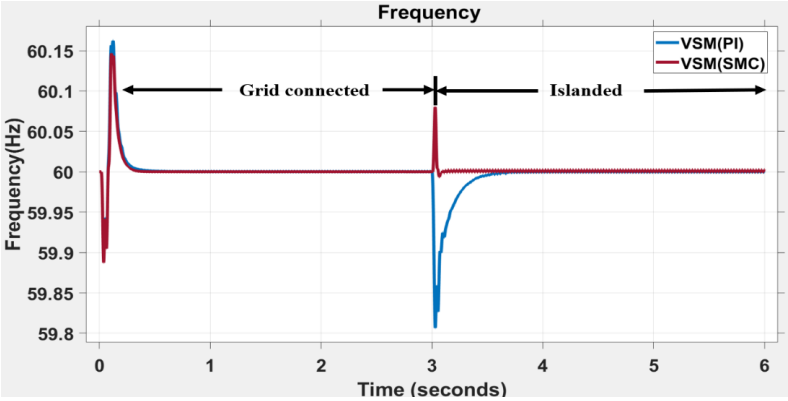

Fig.8 System frequency

Figure 8 illustrates the system frequency response over time for two different control strategies in a Virtual Synchronous Machine with SMC and without SMC. During the grid-connected mode from 0s to 3s, both controllers maintain the system frequency close to 60 Hz, with less oscillations. However, the VSM with SMC stabilizes better when compared to the VSM with SMC control. At 3s, when the system transitions from grid-connected to islanded mode, the VSM without SMC experiences a significant frequency dip below 59.85 Hz, taking 0.6ms to recover. In contrast, the VSM with SMC shows only a small transient at 60.07Hz and within 0.1ms its settles back to 60 Hz. During the islanded mode from 3s to 6s, both controllers maintain the frequency, but the SMC-based VSM ensures better stability and a quicker response. This analysis demonstrates that the Sliding Mode Controller (SMC) significantly enhances the robustness of the VSM, reducing frequency deviations and ensuring a more stable transition compared to the traditional PI controller.

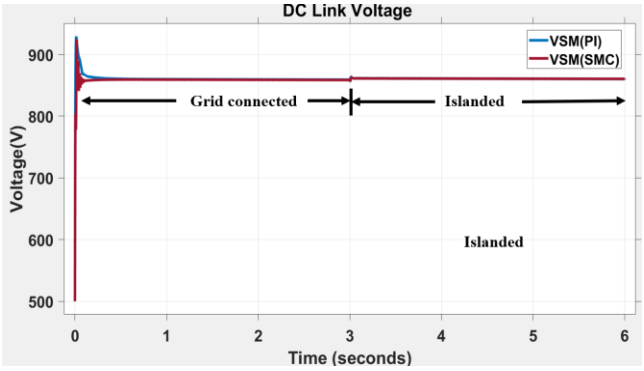

Fig.9 DC Link voltage Graph

The transition from grid-connected mode to islanded mode is shown in Figure 9. Initially, during the grid-connected mode from 0s to 3s, both controllers regulate the DC link voltage 860V, with less transient oscillations. The VSM without SMC voltage settled at 0.3ms and VSM with SMC settled at 0.1ms, The VSM with SMC shows a faster stabilization compared to the VSM without SMC control. At 3s, when the system transitions from grid-connected to islanded mode, there is a

small disturbance in the voltage, but both controllers maintain stability. However, the VSM with SMC ensures a smoother transition with minimal deviations. During the islanded mode from 3s to 6s, the DC link voltage remains stable, indicating effective voltage regulation by both controllers. The results highlight that the SMC-based VSM provides improved transient performance and quicker settling time compared to the traditional PI-based VSM, making it more robust in handling system disturbances.

Case 2: Fault in line:

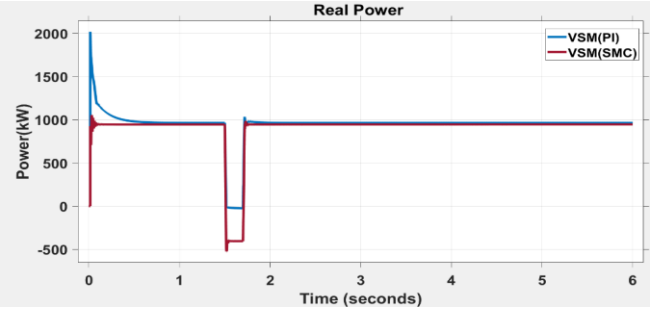

Fig.10 System Real Power

The graph 10 represents the real power response of a Virtual Synchronous Machine (VSM) under two different control strategies. Initially, both controllers regulate power at around 1000 kW, the VSM without SMC controller exhibits a transient overshoot of 2000 kW from the operating power of 900 kW at 0.2 ms. and also, it is settled at 0.6ms. whereas the VSM with SMC controller settled at 0.1ms. the time of from 1.5s to 1.7s, a fault condition occurs, causing a sharp drop in real power. The PI-based VSM struggles with a more pronounced deviation and slower recovery, whereas the SMC-based VSM quickly stabilizes and mitigates oscillations effectively. After the fault is cleared, both controllers restore power regulation, but the SMC-based VSM demonstrates superior robustness and faster recovery. This indicates that the Sliding Mode Controller enhances system stability and dynamic performance, making it more resilient to disturbances compared to the traditional PI based VSM.

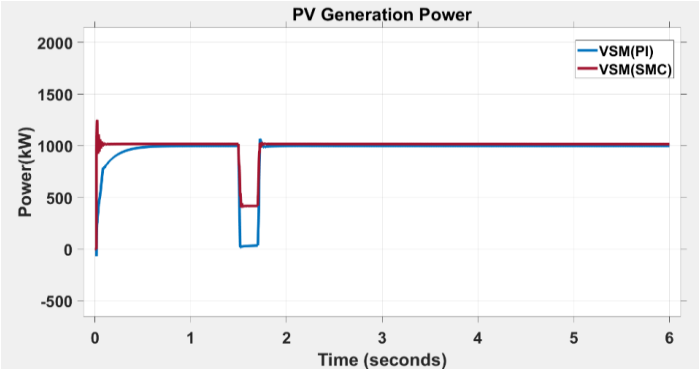

Fig.11 PV Generation Power

This graph 11 illustrates the PV generation power response for VSM with SMC controller and VSM without SMC. Similar to the real power graph, the system initially stabilizes around 1000 kW. The VSM with SMC controller settled at 0.1ms whereas the VSM with SMC controller the takes long time 0.6ms to settled. The VSM without SMC struggles with a more significant power dip and takes longer to recover. In contrast, the SMC-based VSM maintains better stability, experiences a smaller deviation, and quickly restores normal operation after the fault is cleared. This highlights the advantage of Sliding Mode Control in enhancing robustness and ensuring faster fault recovery in a VSM-controlled PV system.

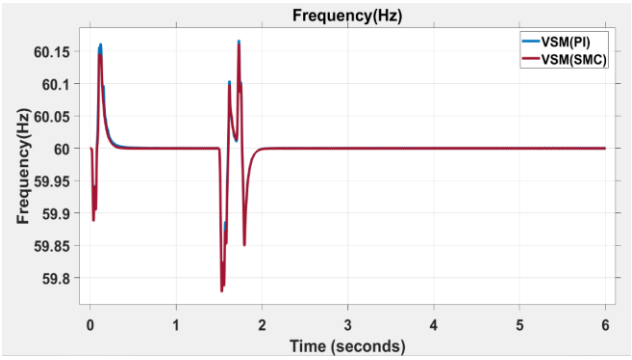

Fig.12. System Frequency

Figure 12 shows the frequency response of the system for VSM without SMC and VSM with SMC. Initially Both controllers experience an overshoot, but the VSM with SMC exhibits small switching transient compare to Without SMC. And faster settling time and better damping. The SMC-controlled system experiences oscillations but restores stability faster than without the SMC controlled system. Both controllers return to a steady-state frequency

of approximately 60 Hz, but SMC ensures a quicker and more stable response. This confirms that SMC enhances system robustness by reducing the effect of frequency disturbances and improving stability, making it a better choice for grid-forming VSM applications.

Case 3: Varying irradiation in solar PV:

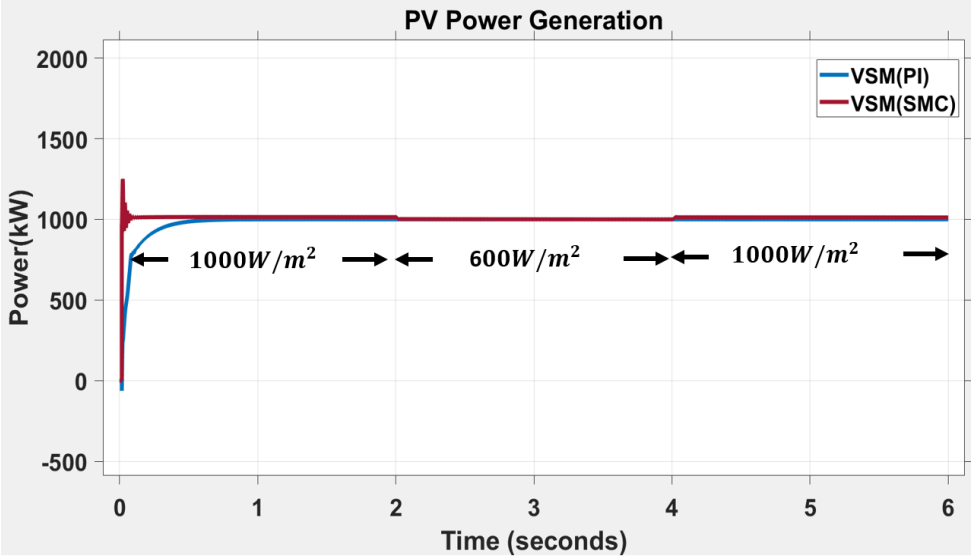

Fig.13 Pv generation power

When irradiance is 1 000W/m² (0–2 s), the SMC-based VSM settles in about 0.1s, whereas the PI based VSM takes 0.6s to converge. At 2s the irradiance drops to 600W/m², both controllers track the lower power smoothly. When sunlight returns to 1000W/m² at 4s, again both the controllers start tracking their reference 1MW without any disturbance. These results confirm the SMC strategy's superior transient response and robustness to rapid irradiance changes.

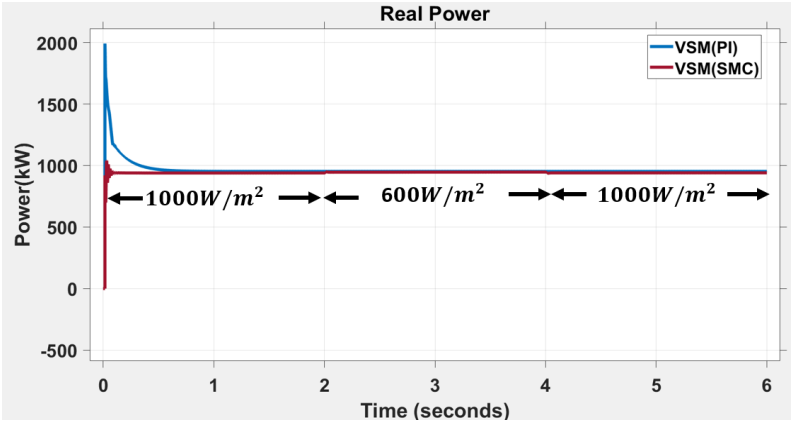

Fig.14 System Real power

Under variable irradiance conditions, the real power output of the VSM controlled system demonstrates the effectiveness of both controllers. At the initial irradiance of 1000 W/m² (0–2 s), the SMC based VSM reaches steady-state within 0.1s, showing minimal overshoot. In contrast, the PI controlled VSM exhibits a significant overshoot up to 1900kW and takes about 0.6 s to stabilize. As the irradiance drops to 600W/m² at 2s, both controllers adjust accordingly. When irradiance returns to 1000 W/m² at 4s, both the controller resynchronized quickly without any disturbance. These observations confirm the superior transient performance and robustness of the SMC based VSM in real power control.

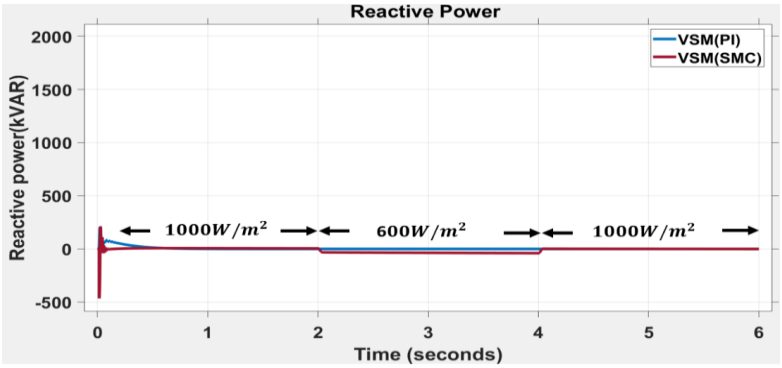

Fig.15 system reactive power

Under variable irradiance conditions, the reactive power response of the VSM controlled system highlights the performance differences between the two controllers. At the initial irradiance of 1000W/m² (0–2s), the SMC-based VSM reaches reactive power steady state quickly with minimal fluctuation, while the PI based VSM shows a slower response with a slight overshoot around 100kVAR. When irradiance drops to 600 W/m² at 2s, both controllers adjust smoothly.

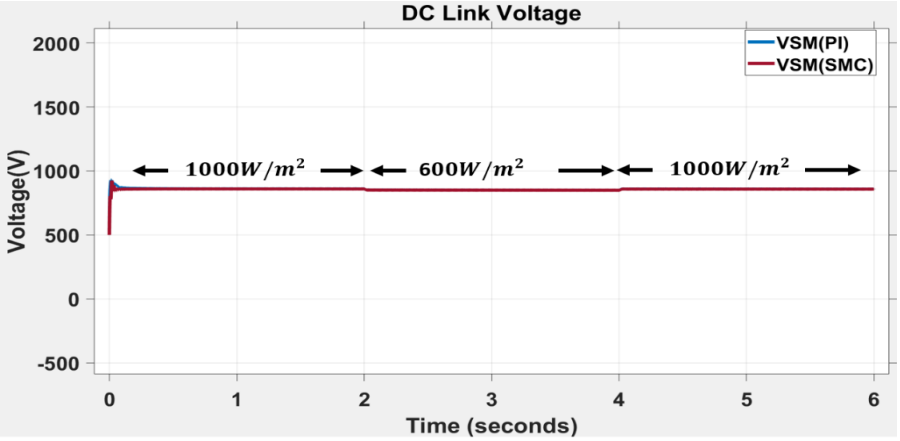

Fig 16 DC link voltage

Under varying irradiance, the DC link voltage performance demonstrates the voltage regulation capabilities of both controllers. At an initial irradiance of 1000 W/m² (0–2 s), both controllers stabilize the voltage near the reference value 800V with minimal transients. The SMC based VSM reaches steady-state faster and with slightly less fluctuation compared to the PI based VSM. As irradiance drops to 600 W/m² at 2s, both controllers effectively maintain voltage stability. When irradiance returns to 1000 W/m² at 4s, the voltage remains tightly regulated in both cases.

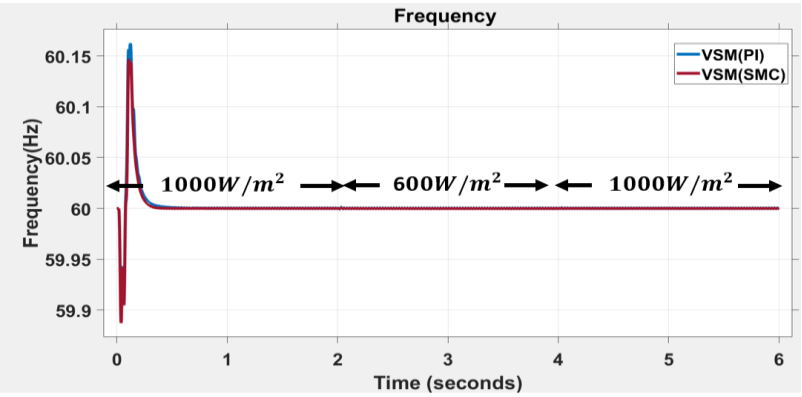

Fig 17 System frequency

Under variable irradiance, the frequency dynamics of the VSM controlled system reveal the controller's transient performance. At an initial irradiance of 1000 W/m² (0–2s), the SMC based VSM quickly settles near 60Hz within 0.15s. The PI controlled VSM exhibits a slower and more oscillatory response, taking about 0.2s to stabilize. As the irradiance drops to 600 W/m² at 2s, and returns to 1000 W/m² at 4sec, both controllers maintain frequency close to the nominal value. However, the SMC controller continues to demonstrate faster damping and minimal deviation, confirming its superior frequency regulation and dynamic robustness.

Case 4: Islanded to grid mode:

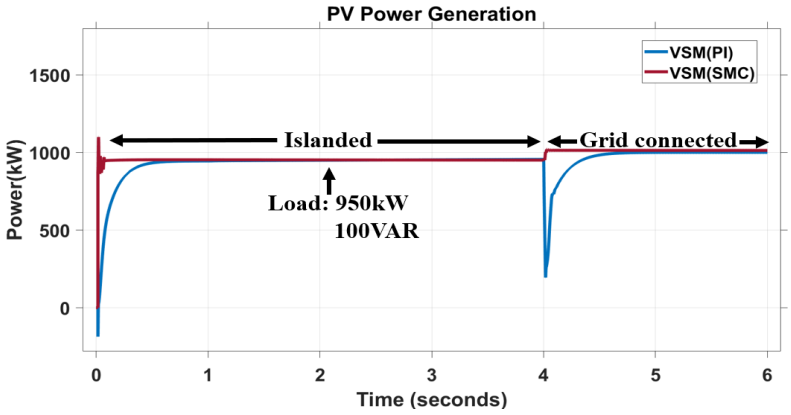

Fig.18 PV generation power

During the islanded mode as shown in fig 18, both controllers maintain power close to the load demand of 950 kW and 100 VAR. The VSM with SMC settles in about 0.1s, whereas the PI controlled VSM takes around 0.6s. When the system is connected to grid connected mode The PI based VSM experiences a sharp transient, dipping to about 200 kW and requiring 0.6s to resynchronize. In contrast, the SMC based VSM control shows a much smoother response and settles within 0.1s. These results demonstrate the superior stability and robustness of the SMC based VSM approach during both steady state operation and transition phases, confirming its effectiveness in handling sudden mode changes in grid forming microgrid.

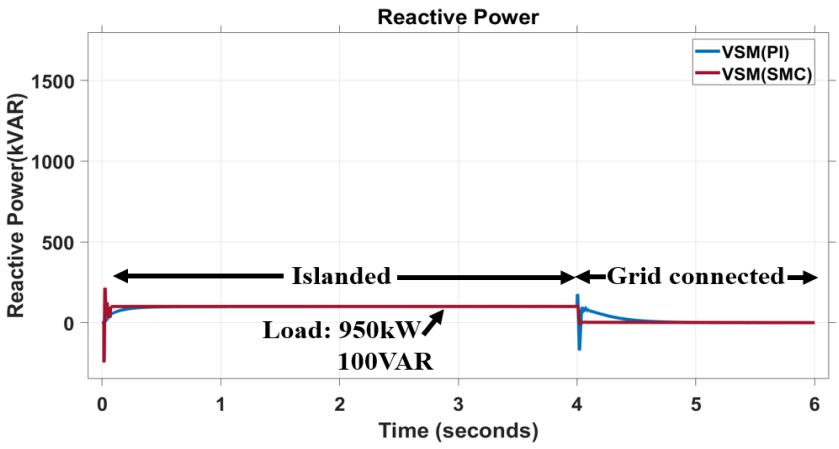

Figure 19. Reactive power of inverter

During the islanded mode as shown in figure 19, both controllers regulate reactive power close to the load demand of 100 VAR and 950kW. The VSM with SMC settled at 0.1s, while the PI-controlled VSM takes 0.2s to reach steady state. At 4s, when the microgrid reconnects to the

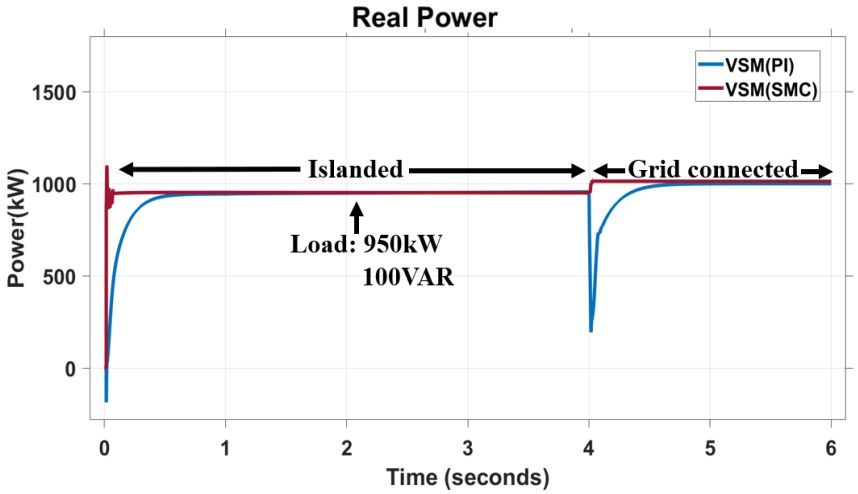

utility, the PI based VSM experiences a pronounced transient, spiking to 150 kVAR and then settling at 0.6s. In contrast, the SMC based VSM shows only a slight disturbance and resettles within 0.1s. These results underscore the superior damping and faster dynamic response of the SMC based VSM strategy during both steady operation and grid transition events.

Figure 20.System Real power

During the islanded mode as shown in fig 20, both controllers provide 950 kW and 100VAR demand through the VSM with SMC which settles in 0.1s, whereas the PI controlled VSM takes 0.6s to settle. The PI controlled VSM encountered a switching transient of 300 kW and then takes another 0.6s to regain steady output. By contrast, the SMC based VSM shows only a slight perturbation and resettles within 0.1 s. These results confirm the SMC strategy's faster response, superior disturbance rejection, and overall robustness during both steady operation and grid-transition events.

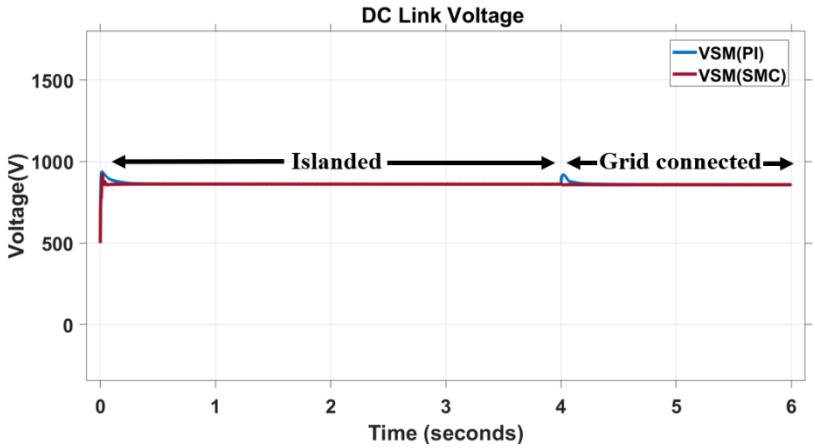

Figure.21 DC link voltage

Initially, in the islanded operating mode shown in fig 21, both controllers maintain the DC link voltage close to its reference as 800V. The SMC based VSM stabilizes the voltage rapidly within 0.1 seconds, whereas the PI controlled VSM exhibits a slightly slower settling around 0.3s. At the transition point to grid connected mode at 4s the PI based VSM controller experiences a voltage overshoot, while the SMC based VSM maintains a more stable and smoother response. This demonstrates the superior voltage regulation and transient handling capability of the SMC based VSM under dynamic operating conditions.

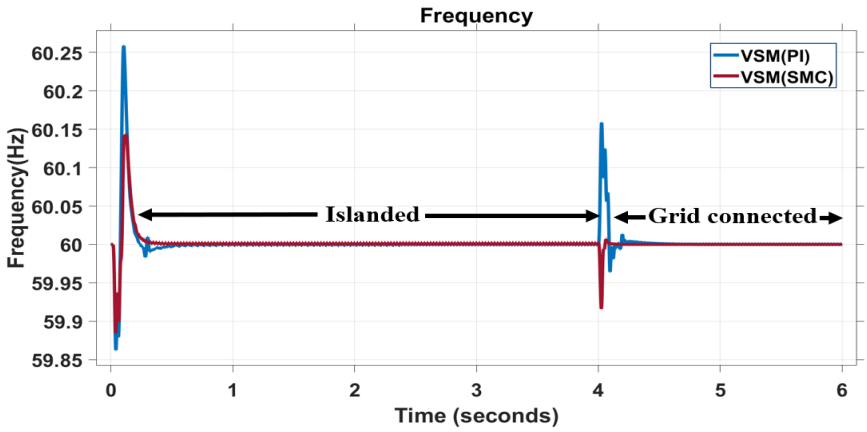

Figure 22 System Frequency Graph

At the onset of islanded operation 0 -4 s, as shown in Figure 22, both controllers operate at the 60Hz reference. The SMC based VSM damps oscillations within approximately 0.1s, whereas the PI controlled VSM takes around 0.3s. At 0.1s, the SMC based VSM creates a switching transient slightly above 60Hz, reaching 60.15Hz. In contrast, the PI based VSM causes a transient reaching up to 60.25Hz however, both remain within the acceptable operating region. When the microgrid reconnects to the grid at 4s, the PI-controlled VSM exhibits a pronounced frequency spike above

60.15Hz and several oscillatory swings before settling. In contrast, the SMC based VSM maintains a small deviation and resynchronizes in under 0.1s. These results highlight the SMC strategy's superior damping and faster frequency stabilization during both steady operation and grid transition events.

6. Hardware Implementation

The final system was partially deployed on hardware with FPGA generating control pulses. Power stages including the boost converter and inverter were tested with lab-scale PV sources and BESS.

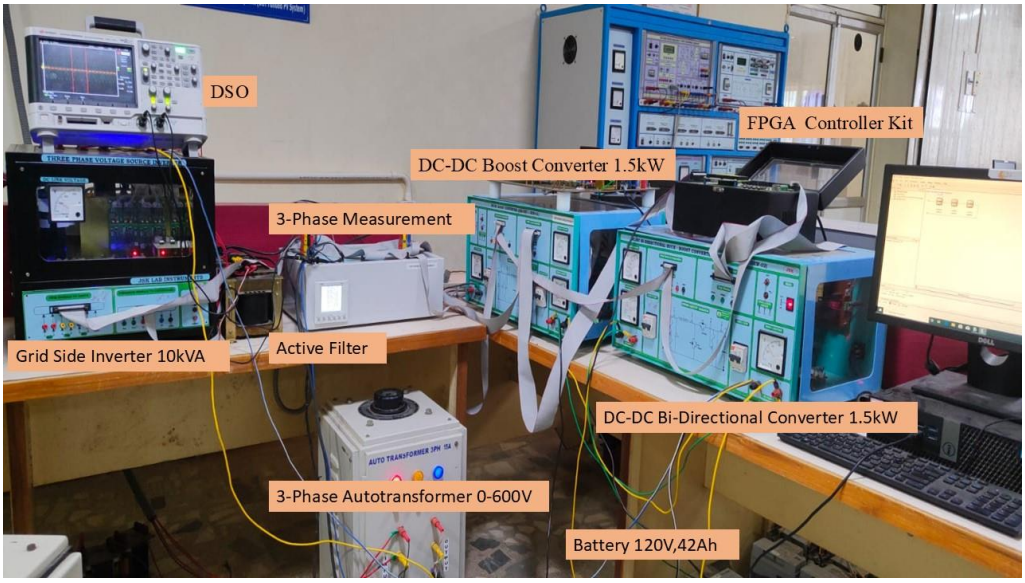

Figure 23.Microgrid Setup with Solar PV-BESS integrated with Grid

Figure 23 illustrates the implementation of GFM- and GFL-based inverter control techniques on a 1 kW grid-tied PV-BESS microgrid hardware configuration. The system's components included solar PV panels, battery energy storage, a boost converter, FPGA processor boards (SPARTAN-6), an inverter module, a bidirectional converter, a grid sensor module, a three-phase autotransformer, and grid interface components. A reference voltage is set using the FPGA processor board to regulate inverter operation. The AC output of the inverter was interfaced to the grid via an autotransformer. Voltage and current measurements on both the AC and DC sides were taken using voltage and current sensors, with data captured using a digital storage oscilloscope (DSO) To evaluate system robustness, grid faults were simulated by adjusting the

isolation transformer, causing voltage dips and surges to emulate both low and high voltage grid conditions.

7. Conclusion

This project demonstrates the implementation of a Sliding Mode Controller (SMC) integrated with a Virtual Synchronous Machine (VSM) for enhancing the stability of a grid forming inverter in a PV-BESS based microgrid system. The simulation was carried out for a 1MW system, while the practical hardware implementation was tested on a 1kW setup. The effectiveness of the proposed SMC based VSM strategy was validated under four critical operating scenarios such as grid-connected to islanded mode transition, occurrence of a short-circuit fault, variation in solar irradiance, and islanded to grid reconnection. Across all these cases, the SMC based VSM significantly reduced switching transients and achieved faster resynchronization compared to traditional grid forming controllers such as droop control and PI based VSM control. Frequency and voltage overshoots were limited to within 0.05 Hz and 2%, respectively, while real power dips remained below 50 kW. The system consistently achieved settling times of less than 0.1 seconds in the simulation. These results confirm that the non-linear sliding surface provides high-gain robustness without sacrificing the inertial emulation benefits of VSM. Therefore It successfully dampens transient spikes, improves system resilience, and ensures smoother transitions. Therefore, the proposed SMC based VSM strategy provides a promising, scalable, and hardware compatible solution for robust and reliable operation of future microgrids under dynamic and fault-prone conditions.

8. My Role in the Project

- Developed a grid-connected microgrid system integrating solar PV and battery energy storage.
- Implemented Grid-Forming (Droop, Virtual Synchronous Machine) and Grid-Following inverter control strategies.
- Designed and tested an adaptive Sliding Mode Controller to minimize oscillations during voltage/current tracking.
- Simulated the control strategies in MATLAB and validated them under variable load and fault conditions.

- Converted the controller logic to VHDL and implemented PWM control using Xilinx FPGA hardware.
- Designed hardware using KiCad including a bidirectional DC-DC converter and inverter PCB.
- Validated hardware and controller performance for a 1 kW microgrid setup in both simulation and real-time testing.